Ab Initio Study of the Photochemistry of c-C_2H_2Si

Masae Takahashi*,† and Kenkichi Sakamoto‡

Photodynamics Research Center, RIKEN (The Institute of Physical and Chemical Research), 519-1399 Aoba, Aramaki, Aoba-ku, Sendai 980-0845, Japan

Received: April 9, 2004; In Final Form: June 30, 2004

The photochemical reaction pathway of silacyclopropenylidene (c-C_2H_2Si) has been investigated using the eight electrons in eight orbitals complete active space with the 6-311++G(3df,3pd) basis sets. The mechanism of drastic structural change in the reaction of c-C_2H_2Si and the difference from the reaction of cyclyopropenylidene (c-C_3H_2) are elucidated. The photochemically active relaxation path of c-C_2H_2Si on the S_1 excited-state potential surface leads to an S_1/S_0 conical intersection where the photoexcited system decays nonradiatively to S_0. The relaxation of c-C_2H_2Si on the S_1 surface causes the cleavage of the Si−C single bond, while that of c-C_3H_2 causes the cleavage of the C−C double bond. The difference in photochemical cleavage sites is well explained by the difference in the electronic nature of the S_1 excited state. In the dark reaction following the relaxation on the S_1 surface, hydrogen migration from carbon to silicon occurs together with ring opening at the Si−C bond.

Introduction

Cyclopropenylidene (**1**, *c*-C_3H_2) is abundant in molecular clouds of interstellar space and has been shown to play a decisive role in the chemistry of interstellar clouds.[1−4] The silicon analogue, silacyclopropenylidene (**3**, *c*-C_2H_2Si), would also be of interest particularly in astrochemistry and structural chemistry.[5] Maier et al. have reported the synthesis and the photoisomerization of **1** and **3**.[6,7] In those papers, it was shown that photochemical interconversion of **1** occurred between three C_3H_2 isomers: **1**, propargylene (**2**), and vinylidenecarbene.[6] On the other hand, the photochemical reaction of **3** is complicated, and several isomers were detected during the reaction.[7] Each isomer observed in the photochemical reaction of **3** has been attracting the interest of theoretical chemists.[8−14] The reaction product detected by infrared (IR) spectroscopy is **2** and **4** with irradiation of 254 nm light[6] to **1** and **4** and with that of 313 nm light to **3**[7] (Scheme 1), respectively. The ring opening of **3** at the C═C and Si−C bonds yields compounds **5** and **6**, respectively, but not compound **4**. Compound **5** contains a singlet carbene part and a Si≡C triple bond part and thus is an attractive target of synthesis. To clarify the photochemical reaction pathway leading to **4**, theoretical investigation is necessary. Despite numerous studies of the structures of C_2H_2-Si species, no theoretical investigation of the photochemical reaction pathways of C_2H_2Si has been reported.

Photochemical reaction consists of three successive processes: vertical excitation by a photon, relaxation on an excited-state potential surface, and dark reaction on a ground-state potential surface. The first process decides the excited-state surface on which the following reaction proceeds and thus should be investigated carefully. From the comparison between calculated UV absorption wavelengths and the excitation wavelength used in the experiments, the excited state is determined. Accurate calculations of UV absorption wavelengths are required. In our previous studies, we calculated UV absorption maxima of several disilene and silylene derivatives,[15−17] and found a good linear correlation between experiments and calculations (correlation coefficient 0.98). We apply the correlation to the present silylene, **3**, and reveal the first event of the photochemistry of **3**, and then we investigate the successive photochemical reaction of **3** using the complete active space (CAS) method.[18,19]

SCHEME 1: Photochemical Reactions of 1 and 3

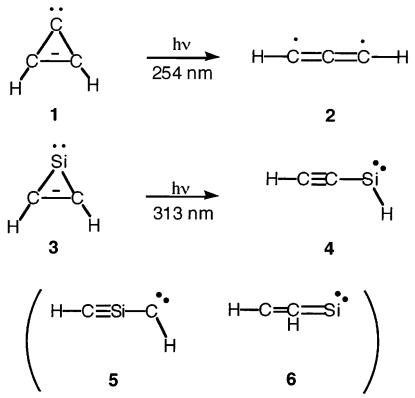

Calculations

Ab initio molecular orbital calculations were performed using the Gaussian 98 software package.[20,21]

UV absorption maxima were calculated at the TD/6-311++G(d,p)//MP2/6-31G(d) level, and the calculated values X (eV) were corrected to Y (eV) with a correlation line for organosilicon compounds: $Y\,(\mathrm{eV}) = 0.78[X\,(\mathrm{eV})] + 0.52$.[15−17] The calculation level we use here to obtain UV absorption maxima is the same as that used in refs 15 and 16 to obtain the correlation line.

† Present address: Institute for Materials Research, Tohoku University, Sendai 980-8577, Japan.

‡ Concurrent office: Department of Chemistry, Graduate School of Science, Tohoku University, Aoba-ku, Sendai 980-8578, Japan.

10.1021/jp048424t CCC: $27.50
Published on Web 08/06/2004

In the investigation of photochemical reaction pathways, the eight electrons in eight orbitals CAS method[18,19] was used with the 6-311++G(3df,3dp) basis sets for geometry optimization. In our preceding study on organosilicon compounds, excellent results were obtained using the 6-311++G(d,p) basis set.[22] However, the addition of high-exponent d and f inner polarization functions was found to be essential for obtaining reliable geometries of second-row species in some cases.[23,24] For several organosilicon compounds, maximum and average differences in bond length between MP2/6-311+G(3df,2p) and B3LYP/6-311++G(d,p) calculations are 0.029 and 0.007 Å, respectively.[25] In the present study, the C−Si bond distances are longer by 0.007−0.008 Å at the CAS/6-311++G(d,p) level than that at the CAS/6-311++G(3df,3pd) level. An accurate bond distance seems crucial for the study of bond-cleavage reaction on the excited-state surface. Therefore, we used the 6-311++G(3df,3pd) basis sets. Energies were calculated at the MP2-CAS(8,8)/6-311++G(3df,3pd) level using CAS(8,8)/6-311++G(3df,3pd) geometry.

It is common understanding that the selection of correct orbitals for the active space should be carefully carried out in the photochemical study using CASSCF methods. According to the tutorial[26] for examining the orbitals and planning the active space, we first examine the natural orbitals. We selected a π_{CC} orbital, two σ_{SiC} orbitals, and a lone-pair orbital. We must give some justification of the use of the eight active orbitals to describe the present system. As mentioned in the Results and Discussion, the first allowed band is best described as n → 3p(Si). The carbon π orbital (π_{CC}) is mixed in an antibonding manner with the 3p(Si) orbital. The photochemical reaction treated here is the Si−C bond cleavage. Consequently, a π_{CC} orbital, two σ_{SiC} orbitals, and a lone-pair orbital at silicon were selected.

Minima and transition states were confirmed by the calculations of harmonic vibrational frequencies in both UV and reaction-path studies. Reaction pathways from transition states were followed by intrinsic reaction coordinate (IRC) calculations.

Results and Discussion

First, the excited state produced by the irradiation of 313 nm light to **3** and its electronic nature are revealed, on the basis of the accurate calculations of UV absorption wavelengths at the TD/6-311++G(d,p)//MP2/6-31G(d) level with correction using a correlation line for organosilicon compounds. The vertical excitation energy to the lowest excited state (S_1) of **3** was calculated to be 4.79 eV with an oscillator strength of 0.097 at the TD/6-311++G(d,p)//MP2/6-31G(d) level. In the calculation, the geometry was fully optimized at the MP2/6-31G(d) level, and the minimum structure has C_{2v} symmetry. After correction using the correlation line for organosilicon compounds, the corresponding absorption band is at 291 nm. The calculated 291 nm band for **3** is best described as the n → 3p(Si) transition. The UV measurement of **3** shows a weak, broad absorption between 260 and 320 nm (λ_{max} = 286 nm),[7] which is in good agreement with our calculations on the wavelength and the weak oscillator strength. The next allowed band is calculated to be 227 nm after correction using the correlation line, and the oscillator strength is 0.028. The second band is well separated from the first band and has much less oscillator strength. These results suggest that photoexcitation of **3** with 313 nm light leads to the lowest excited state ^{1}(n → 3p). Between the first and second bands, a forbidden band (the oscillator strength is zero) exists and the vertical excitation energy is 4.80 eV, which is very close to the energy of the first band. The electronic nature of the forbidden transition is σ_{CSi} → 3p(Si). Since the vertical excitation energy of the forbidden band is very close to that of the lowest allowed band, the excited state should be carefully chosen in the following calculation of relaxation on the excited-state surface using the CASSCF method.

TABLE 1: Molecular Structure of c-C_2H_2Si

	bond distance (Å)			bond angle (deg)
	r(C−C)	r(C−Si)	r(C−H)	∠(C−C−H)
		This Work		
C_{2v} structure	1.341	1.837	1.072	135.6
C_s structure	1.342	1.833, 1.805	1.072, 1.093	134.4, 134.6
MW (r_s)[a]	1.3458	1.8200	1.0795	135.16
		Δ(calcd − obsd)		
		This Work		
C_{2v} structure	0.005	−0.017	−0.008	0.4
C_s structure	−0.004	0.013, −0.017	−0.008, 0.013	−0.8, −0.6
		Previous Work		
DZ+PSCF[b]	−0.003	−0.014	−0.002	−1.0
CASSCF/TZVP[c]	−0.011	−0.007	−0.007	−1.1
MP2/DZP[d]	0.014	0.012	0.005	0.6
CISD/TZ2P[e]	−0.007	−0.003	−0.006	−0.8
CCSD(T)/TZ(2df,2pd)[f]	0.004	0.013	0.002	0.1

[a] Reference 27. [b] Reference 10. [c] Reference 12. [d] Reference 11. [e] Reference 13. [f] Reference 14.

Second, the excited-state surface on which relaxation proceeds at the CAS(8,8)/6-311++G(3df,3pd) level is selected. Geometry optimization of **3** gives two minimum structures with different symmetries, C_s and C_{2v}, at the CAS(8,8)/6-311++G(3df,3pd) level of calculations, while one minimum structure with C_{2v} symmetry is obtained at the MP2/6-31G(d) level of calculations as mentioned above. The optimized C_{2v} structure is more stable than the C_s structure by 1.9 kcal/mol at the CAS(8,8)/6-311++G(3df,3dp) level, but a little bit less stable by 0.3 kcal/mol at the MP2-CAS(8,8)/6-311++G(3df,3pd) level. Izuha et al. determined the precise molecular structure of **3** from observed rotational constants of its isotopic species in their microwave spectral study.[27] Optimized geometric parameters of C_s and C_{2v} structures in our present study are compared with the experimental data[27] and results of previous calculations[10−14] (Table 1). The calculated C−Si bond length of the C_s structure shows better agreement on the average with the experimental value than that of the C_{2v} structure. The discrepancies of the bond lengths of C═C and C−H and the C−C−H bond angle from the experimental values are similar to each other in the two structures. From the final one-electron symbolic density matrix obtained at the CAS(8,8)/6-311++G(3df,3pd) level of calculations, the electronic nature of the S_1 excited states of both C_s and C_{2v} structures is ^{1}(n → 3p) and the vertical transition of two structures to the S_1 excited state is allowed. The absorption wavelength (the energy difference between the S_0 and S_1 states) of the C_s structure is 290 nm at the CAS(8,8)/6-311++G(3df,3pd) level, and that of the C_{2v} structure is 289 nm. At the MP2-CAS(8,8) level, those values are 295 and 300 nm for the C_s and C_{2v} structures, respectively. Both calculated absorption wavelengths are in excellent agreement with the experimental value of 286 nm. Although none of the previous theoretical studies have located the C_s symmetry[10−14] and the C_s minimum may be an artifact of the CASSCF method, we use the S_1 excited-state surface of the C_s structure in the calculation of photochemical reaction pathways at the CAS(8,8)/6-311++G-

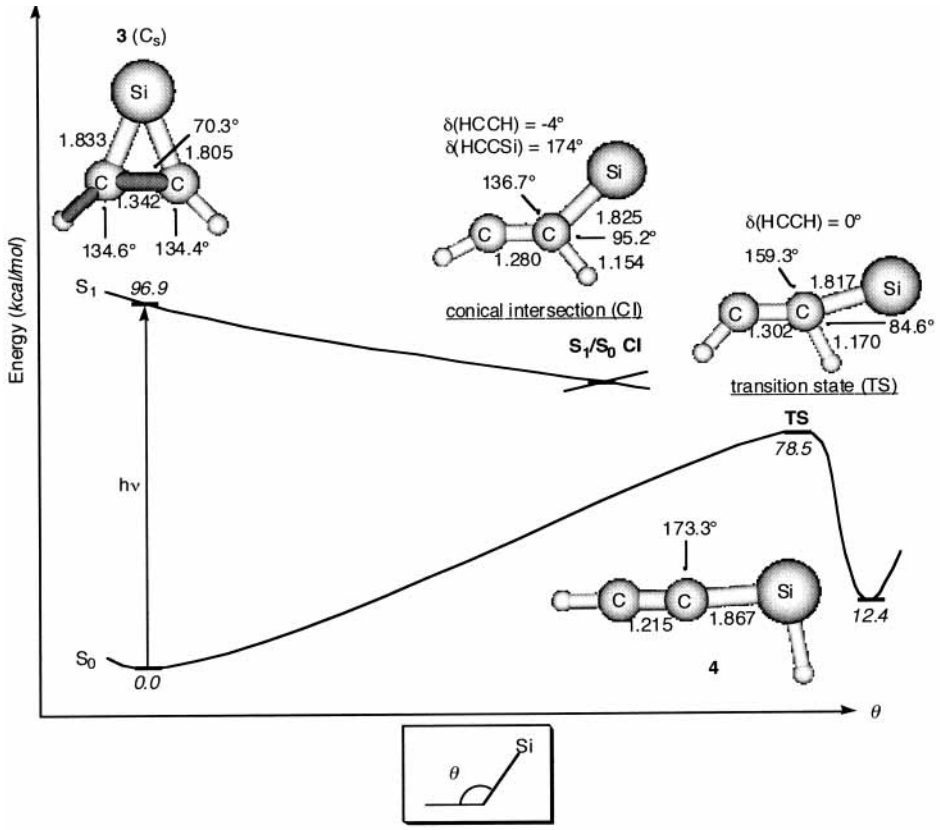

Figure 1. Potential energy diagram for the photochemical reaction of **3** with C_s symmetry versus the C−C−Si bond angle (θ) and the CAS(8,8)/6-311++G(3df,3dp)-optimized structures of all stationary points.[29] Energies are the results at the MP2-CAS(8,8)/6-311++G(3df,3pd) level using the CAS(8,8)/6-311++G(3df,3pd) geometry. Bond lengths, bond angles, dihedral angles, and relative energies (italics) are given in angstroms, degrees, degrees, and kilocalories per mole, respectively.

(3df,3pd) level for the following two reasons: (1) the calculated absorption wavelength of 295 nm of the C_s structure obtained at the MP2-CAS(8,8) level gives better agreement with the experimental value than that of 300 nm of the C_{2v} structure; (2) the calculated C−Si bond length of the C_s structure shows better agreement with the experimental value than that of the C_{2v} structure. Although the somewhat better agreement of the C−Si bond length with the experimental value might well be due to better cancellation treatment, an accurate bond distance is important for the study of bond-cleavage reaction on the excited-state surface, and thus, we select the structure having a C−Si bond length closer to the experimental value. Actually, relaxation on an excited-state potential starting from the C_{2v} structure leads to the dissociation to Si + HC≡CH. We are not interested in the dissociation reaction here.

Since the excited state produced by the first process, excitation by a photon, is carefully determined, we next investigate the successive process, relaxation on an excited-state potential surface. The potential energy diagram for the photochemical reaction of **3** and the optimized structures of all stationary points are shown in Figure 1. The energies are given at the MP2-CAS(8,8)/6-311++G(3df,3pd) level using the CAS(8,8)/6-311++G(3df,3pd) geometry. Whole reactions of **3** occur on singlet surfaces, although the reaction pathway of **1** contains a triplet state.[28] **3** is more stable by 12.4 kcal/mol than ethynylsilylene (**4**). The relative stability between **3** and **4** is the same as that of previous theoretical studies.[10] Geometry optimization on the S_1 $^1(n \rightarrow 3p)$ excited state is performed from the C_s structure of **3**. The relaxation reaches an S_1/S_0 conical intersection (CI) where the photoexcited system decays nonradiatively to S_0. That is, the photochemically active relaxation path starting from the S_1 $^1(n \rightarrow 3p)$ excited state of the C_s structure of **3** leads to the S_1/S_0 CI.[29] One Si−C bond length is elongated to 2.894 Å at the S_1/S_0 CI. From the structure at the S_1/S_0 CI, the nature of the relaxation path on the S_1 potential surface is regarded as Si−C bond cleavage. The S_1/S_0 CI-like structure was not found in the comprehensive study by Frenking et al. on the equilibrium structures of C_2SiH_2 isomers at the DZ+PSCF level.[10] Thermal reaction pathways and several stationary points on excited states of **1** have been reported in detail by Mebel et al. at the CAS-(8,10)/6-31+G(d) level.[28] The nature of the relaxation paths of **1** on the S_1 surface is C═C bond cleavage.[28] It is understandable that the relaxation on the S_1 surface causes C═C bond cleavage for **1** and Si−C bond cleavage for **3**, because the vertical transition is $n \rightarrow \sigma^*_{CC}$ for **1** and $n \rightarrow 3p(Si)$ for **3**. The carbon π orbital is mixed in an antibonding manner with the 3p(Si) orbital of **3**.

Finally, the third process, dark reaction on a ground-state potential surface, is examined. Although photoexcitation raises **3** into an excited electronic state, the products of the photochemical process are controlled by the ground-state (thermal) potential surface. The search for transition states on the S_0 surface near the structure of the S_1/S_0 CI gives a transition state (TS) connecting **3** and **4**.[30] In the thermal (or dark) reaction connecting **3** and **4**, hydrogen migration from carbon to silicon occurs together with ring opening at Si−C bond. The thermal reaction pathway between **3** and **4** and the photochemical reaction pathways are drawn in a two-dimensional map where the horizontal and vertical axes indicate the Si−C bond cleavage by the Si−C−C bond angle (θ) and 1,2-hydrogen rearrangement by the Si−C−H bond angle (δ) (Figure 2). The two-dimensional

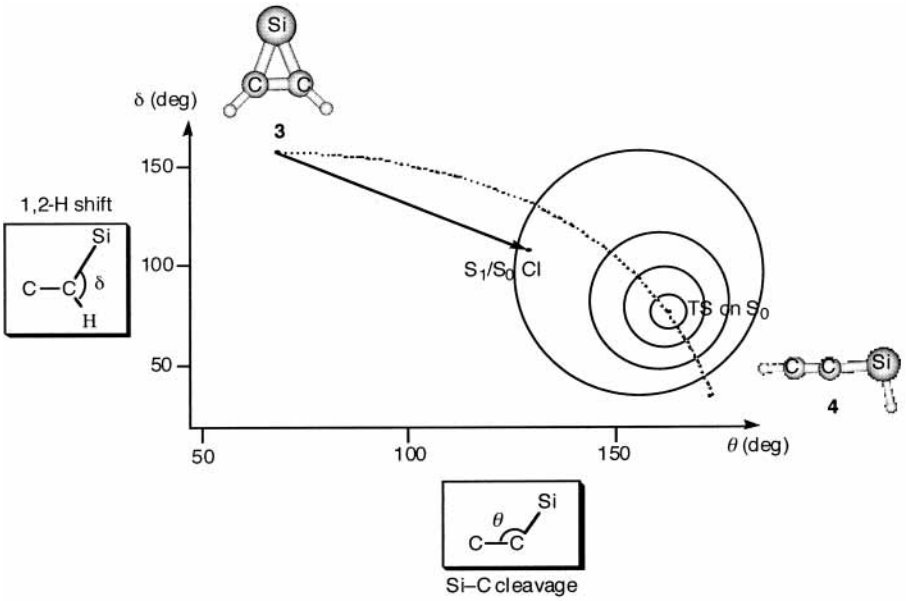

Figure 2. Two-dimensional map for the photochemical (solid line) and thermal (dashed line) reaction pathways of **3**. The horizontal and vertical axes show the C−C−Si and Si−C−H bond angles, respectively.

map makes clear the structural change on ground- and excited-state potential surfaces of these reactions. The S_1/S_0 CI locates near the thermal reaction path. The energy of the TS connecting **3** and **4** on the ground-state potential surface lies 13.3 kcal/mol[31] below the energy of the S_1/S_0 CI. Because of the energy difference, the third process, the reaction on the ground-state potential surface through the S_1/S_0 CI, proceeds over the barrier at the ground-state TS and leads to **4**. Compound **4** is thermodynamically very unstable by 12.4 kcal/mol compared with **3**, but the barrier height between **3** and **4** is quite high (66.2 kcal/mol[32] from **4**). Consequently, it is possible to detect **4** experimentally in photochemical reaction products at room temperature. The ground-state potential profile of **3** is completely different from the profile of **1**. Thermal isomerization of **1** to the singlet HCCCH (**2**) occurs via ring opening at the C═C double bond. Mebel et al. identified a structure similar to the TS connecting **3** and **4** for the carbon analogue as an intersystem-crossing stem of singlet and triplet potential energy surfaces between singlet allene (H_2CCC) and triplet propargylene (HCCCH).[28]

Conclusions

The photochemical reaction pathways of c-C_2H_2Si have been investigated by ab initio calculations at the CAS(8,8)/6-311++G(3df,3pd) level. The difference from the reaction of *c*-C_3H_2, and the mechanism of drastic structural change in the reaction of *c*-C_2H_2Si, is elucidated. The excited state from which the photochemical reaction proceeds has been chosen carefully since a forbidden state $^1(\sigma_{CSi} \rightarrow 3p)$ exists energetically close to an allowed state, $^1(n \rightarrow 3p)$. The photochemically active relaxation from the S_1 $^1(n \rightarrow 3p)$ excited state of *c*-C_2H_2Si leads to an S_1/S_0 conical intersection where the photoexcited system decays nonradiatively to S_0. The relaxation on the S_1 surface causes the cleavage of the C−Si single bond, and in the following dark reaction hydrogen migration from carbon to silicon occurs together with ring opening.

Acknowledgment. M.T. is grateful to Hayashi Memorial Foundation.

References and Notes

(1) Thaddeus, P.; Vrtilek, J. M.; Gottlieb, C. A. *Astrophys. J.* **1985**, *299*, L63.
(2) Adams, N. G.; Smith, D. *Astrophys. J.* **1987**, *317*, L25.
(3) Cernicharo, J.; Gottlieb, C. A.; Guélin, M.; Killian, T. C.; Paubert, G.; Thaddeus, P.; Vrtilek, J. M. *Astrophys. J.* **1991**, *368*, L39.
(4) Gottlieb, C. A.; Killian, T. C.; Thaddeus, P.; Botschwina, P.; Flügge, J.; Oswald, M. *J. Chem. Phys.* **1993**, *98*, 4478.
(5) Srinivas, R.; Sülzle, D.; Weiske, T.; Schwarz, H. *Int. J. Mass Spectrom. Ion Processes* **1991**, *107*, 369.
(6) Maier, G.; Reisenauer, H. P.; Schwab, W.; Čársky, P.; Hess, B. A., Jr.; Schaad, L. J. *J. Am. Chem. Soc.* **1987**, *109*, 5183.
(7) Maier, G.; Pacl, H.; Reisenauer, H. P.; Meudt, A.; Janoschek, R. *J. Am. Chem. Soc.* **1995**, *117*, 12712.
(8) Saxe, P.; Schaefer, H. F., III. *J. Am. Chem. Soc.* **1980**, *102*, 3239.
(9) Fitzgerald, G.; Schaefer, H. F., III. *Isr. J. Chem.* **1983**, *223*, 93.
(10) Frenking, G.; Remington, R. B.; Schaefer, H. F., III. *J. Am. Chem. Soc.* **1986**, *108*, 2169.
(11) Su, M.-D.; Amos, R. D.; Handy, N. C. *J. Am. Chem. Soc.* **1990**, *112*, 1499.
(12) Cooper, D. L. *Astrophys. J.* **1990**, *354*, 229.
(13) Vacek, G.; Colegrove, B. T.; Schaefer, H. F., III. *J. Am. Chem. Soc.* **1991**, *113*, 3192.
(14) Sherrill, C. D.; Brandow, C. G.; Allen, W. D.; Schaefer, H. F., III. *J. Am. Chem. Soc.* **1996**, *118*, 7158.
(15) Takahashi, M.; Tsutsui, S.; Sakamoto, K.; Kira, M.; Müller, T.; Apeloig, Y. *J. Am. Chem. Soc.* **2001**, *123*, 347.
(16) Takahashi, M.; Kira, M.; Sakamoto, K.; Müller, T.; Apeloig, Y. *J. Comput. Chem.* **2001**, *22*, 1536.
(17) In refs 15 and 16, we reported erroneously that the UV calculations were carried out at the TD-B3LYP/6-311++G(d,p) level, while they were actually carried out at the TD/6-311++G(d,p) level.
(18) Bernardi, F.; Olivucci, M.; Robb, M. A. *Chem. Soc. Rev.* **1996**, *25*, 321.
(19) Bernardi, F.; Olivucci, M.; Michl, J.; Robb, M. A. *Spectrum* **1996**, *9*, 1.
(20) Hehre, W. J.; Radom, L.; Schleyer, P. v. R.; Pople, J. A. *Ab Initio Molecular Orbital Theory*; Wiley: New York, 1986.
(21) All calculations were performed with Gaussian 98, revision A11, Gaussian, Inc., Pittsburgh, PA, 2001: Frisch, M. J.; Trucks, G. W.; Schlegel, H. B.; Scuseria, G. E.; Robb, M. A.; Cheeseman, J. R.; Zakrzewski, V. G.; Montgomery, J. A.; Stratmann, R. E., Jr.; Burant, J. C.; Dapprich, S.; Millam, J. M.; Daniels, A. D.; Kudin, K. N.; Strain, M. C.; Farkas, O.; Tomasi, J.; Barone, V.; Cossi, M.; Cammi, R.; Mennucci, B.; Pomelli, C.; Adamo, C.; Clifford, S.; Ochterski, J.; Petersson, G. A.; Ayala, P. Y.; Cui, Q.; Morokuma, K.; Salvador, P.; Dannenberg, J. J.; Malick, D. K.; Rabuck, A. D.; Raghavachari, K.; Foresman, J. B.; Cioslowski, J.; Ortiz, J. V.; Baboul, A. G.; Stefanov, B. B.; Liu, G.; Liashenko, A.; Piskorz, P.; Komaromi, I.; Gomperts, R.; Martin, R. L.; Fox, D. J.; Keith, T.; Al-Laham, M. A.; Peng, C. Y.; Nanayakkara, A.; Challacombe, M.; Gill, P. M. W.; Johnson, B.; Chen, W.; Wong, M. W.; Andres, J. L.; Gonzalez, C.; Head-Gordon, M.; Replogle, E. S.; Pople, J. A.

(22) Veszprémi, T.; Takahashi, M.; Hajgató, B.; Kira, M. *J. Am. Chem. Soc.* **2001**, *123*, 6629.
(23) Bauschlicher, C. W., Jr.; Partridge, H. *Chem. Phys. Lett.* **1995**, *240*, 533.
(24) Martin, J. M. L. *J. Chem. Phys.* **1998**, *108*, 2791.
(25) Takahashi, M.; Sakamoto, K. *Organometallics*, **2002**, *21*, 4212.
(26) Foresman, J. B.; Frisch, Æ. *Exploring Chemistry with Electronic Structure Methods*; Gaussian, Inc.: Pittsburgh, PA, 1993.
(27) Izuha, M.; Yamamoto, S.; Saito, S. *Can. J. Phys*. **1994**, *72*, 1206.
(28) Mebel, A. M.; Jackson, W. M.; Chang, A. H. H.; Lin, S. H. *J. Am. Chem. Soc.* **1998**, *120*, 5751.
(29) It takes too much time with our computer system to optimize the excited-state geometry at the CAS(8,8)/6-311++G(3df,3pd) level. First, several optimization steps at the CAS(8,8)/6-311++G(3df,3pd) level give a structural change similar to that of the optimization steps at the CAS-(6,6)/6-311++G(3df,3pd) level. Both indicate the Si−C bond cleavage. Therefore, we get through with the optimization on the excited-state surface at the CAS(6,6)/6-311++G(3df,3pd) level. At the CAS(6,6)/6-311++G-(3df,3pd) level, the CI lies higher by 13.3 kcal/mol than the TS and lower by 24.7 kcal/mol than the vertical excited state.
(30) At the CAS(6,6)/6-311++G(3df,3pd) level, we obtain the transition state connecting **3** and **4**. However, we obtain a local minimum at the CAS-(8,8)/6-311++G(3df,3pd) level, but the structure is similar to the TS at the CAS(6,6)/6-311++G(3df,3pd) level. Probably the potential surface is shallow at the CAS(8,8)/6-311++G(3df,3pd) level, and the energy and structure of the minimum seem to be very close to those of the TS.
(31) Results at the CAS(6,6)/6-311++G(3df,3pd) level.
(32) Energy difference between the local minimum close to the TS and **4**.